

The properties of strange quark matter and evolution of strange quark stars

Huai-Min Chen,^{1,*} Cheng-Jun Xia², and Guang-Xiong Peng^{3,4,5}

¹*School of Mechanical and Electrical Engineering, Wuyi University, Wuyishan 354300, China*

²*Center for Gravitation and Cosmology, College of Physical Science and Technology, Yangzhou University, Yangzhou 225009, China*

³*School of Nuclear Science and Technology, University of Chinese Academy of Sciences, Beijing 100049, China*

⁴*Theoretical Physics Center for Science Facilities, Institute of High Energy Physics, P.O. Box 918, Beijing 100049, China*

⁵*Synergetic Innovation Center for Quantum Effects and Application, Hunan Normal University, Changsha 410081, China*

In this work, we study the properties of strange quark matter and reveal the evolution process of strange quark stars employing a self consistent thermodynamic treatment. A comprehensive and reliable thermodynamic basis for the study of the dynamic evolution from proto-strange quark stars to stable strange stars at a zero temperature is provided. The relative abundance of particles, equation of state, temperature, and mass-radius relationship at each stage of the evolution of stars are discussed, where the cold strange quark star are consistent with the observational mass and radius of Hess J1731-347, PSR J1231-1411, PSR J0030+0451, PSR J0348+0432, and PSR J0740+6620, which could be difficult to be explained by the standard neutron star model. A schematic diagram is provided as well, illustrating the state of different stages along the evolution of stars at a fixed baryon-mass.

I. INTRODUCTION

Strange quark matter (SQM) is a new form of matter predicted by quantum chromodynamics (QCD), composed of approximately the same number of u, d, and s quarks and a small number of electrons. In the 1970s and 1980s, Witten and Bodmer hypothesized that strange quark matter might be the true ground state of strong interactions [1, 2]. If this is the case, then there must exist objects composed of SQM, such as strange quark stars (SQS) [3, 4], strangelets [5, 6], meteorlike compact ultradense objects [7, 8], and nuclearites [9, 10], etc., which contain the baryons numbers ranging from a few to approximately 10^{57} . For the small lumps of SQM with fewer baryons numbers ($A \leq 10^7$), it is generally referred to as a strangelets [11, 12]. When the size of dense objects composed of SQM reaches the macroscopic scale and becomes a compact star that can be observed by astronomy ($A \approx 10^{57}$), such types of compact stars are called strange quark stars and represent one of the candidates for pulsars [13]. Most subsequent theoretical studies have shown that SQM can exist stably and is more stable than ordinary nuclear matter [14, 15]. Furthermore, it was found that SQM was consistent with the experiments in predicting the phenomena of some strong interaction processes [16, 17]. Therefore, strange quark stars and strangelets consisting of SQM may exist widely in the universe and are expected to be observed.

In general, it is believed that strange quark stars may be directly generated during type II supernova explosions if strange quark matter is absolutely stable. For

example, after a massive star undergoes a supernova explosion, the core of the star is likely to further collapse and form a strange quark star [18]. Meanwhile, ordinary neutron stars may also undergo phase transitions and form strange quark stars. For example, after the annihilation of Weakly Interacting Massive Particles (WIMP) accreted by a regular neutron star, strangelets are generated inside the neutron star, which quickly transform the neutron star into a strange quark star or hybrid star [19]. In fact, as long as there are a trace amounts of strangelets in the universe, all neutron stars have the potential to be transformed into strange quark stars [20, 21]. And it only takes a few milliseconds to convert a neutron star into a strange quark star [22].

The possibility of a core of quark matter inside a neutron star was first explored by Ivanenko and Kurdej-ladze in 1965 [23, 24]. Later, Itoh further developed the notion that dense stars are actually quark stars composed entirely of strange quark matter [25]. Then, many works investigated the dense matter and structure of dense stars [26, 27]. Recently, by considering the isentropic stage of strange quark star evolution, we discussed the structure of pure strange quark stars in the baryon density-dependent quark mass model, and discovered a massive proto-strange quark star with a maximum mass exceeding twice the solar mass, which gave us further insight into the early stages of evolution of a strange quark star [15]. In a theoretical interpretation of observational data from the neutron star EXO 0748-676, Alford's study showed that the presence of quark matter in EXO 0748-676 could not be ruled out [28]. Drake and Slane's research suggests that two hypothetical neutron stars, RXJ 1856.5-3754 in Corona Australis and 3C58 in Cassiopeia, are too small and dense to be neutron stars, and they show the possibility of quark stars [29, 30]. In Ju's work,

* chenhuaimin@wuyiu.edu.cn

they studied the mass-radius relation of HESS J1731-347 based on the MIT bag model, and the results support the hypothesis that HESS J1731-347 is a quark star [31]. In addition, the SN 1987A has so far failed to find a neutron star after core-collapse, and studies have suggested that the dense remnant of SN 1987A may be a strange quark star or strangeon star [32, 33]. The brightest supernova in history, SN 2006gy, exhibited exceptional brightness, being several hundred times brighter than a typical Type II supernova. This abnormally bright supernova indicates that there is a large amount of extra energy, which has led to the suspicion that some kind of quark star may have been born there [34].

As one of the candidates for pulsars, strange quark stars have been studied extensively. In most cases, the theoretical description of strange quark stars is similar to that of neutron stars, i.e., the thermodynamic conditions (e.g., lepton fraction, entropy per baryon, and neutrino chemical potential) are used to study the evolution of strange quark stars [35, 36]. In addition to the baryon density-dependent quark mass model and MIT bag model mentioned above, other phenomenological models have also been applied to the research of strange quark stars, including the Nambu-Jona-Lasinio model [37, 38], quasiparticle model [39, 40], quark-cluster model [41], perturbation model [16, 42, 43], and so on.

In this paper, we apply the baryon density-dependent quark mass model to study the evolution of a strange quark star from a proto-strange quark stars at birth to a stable strange quark star at zero temperature by considering the *beta*-equilibrium matter in the neutrino trapped regime and neutrino transparent regime during the deleptonization and cooling processes of strange quark star. The evolution of proto-strange quark stars involves multiple stages, each with significantly different thermodynamic conditions. By modeling the evolution in stages, the evolution of the strange quark stars can be described more accurately. It is important to note that in any case the modeling results must satisfy the thermodynamic self-consistency, which we have discussed in detail in this paper. By applying a self consistent thermodynamic treatment and requiring the strange quark matter to satisfy the corresponding local electrical neutrality and chemical equilibrium conditions, the relationships between the various thermodynamic quantities of the strange quark matter can be given in a self-consistent way.

The present paper is organized as follow. In Sec. II, we discuss the thermodynamic treatment of SQM with baryon density-dependent quark mass model. In Sec. III, we give the quark and gluon mass scaling at finite and zero temperatures, where the equivalent mass of quarks takes into account confinement and perturbation interactions. In Sec. IV, we present the numerical results for the properties of SQM. In Sec. V, the evolution of a strange quark star are discussed. Finally, a short summary is given in Sec. VI.

II. SELF-CONSISTENT THERMODYNAMIC TREATMENT

The most complex and important issue in the equivalent particle model is thermodynamic self-consistency, in which various thermodynamic treatment have been developed based on different considerations [39, 44, 45]. To introduce the interaction between quarks in a free particle system, the constant quark mass in the thermodynamic expression of the free particle system is replaced with the equivalent mass $m_i = m_i(n_u, n_d, n_s, T)$ that varies with the environment, which alters the relationship between various thermodynamic quantities derived from the original free particle system, and it is necessary to be rederived. In this paper, the free energy density F is taken as the characteristic thermodynamic function, and the expressions of each thermodynamic quantity are obtained by self-consistent thermodynamic treatment. The free energy density adopts the same form as that of the free particle system, but the mass in the expression is replaced by an equivalent mass that depends on density and temperature. Since the objects of interest are bulk strange quark matter and strange quark stars, the independent state parameter are particle number density n_i and temperature T . The free energy density is expressed as

$$\begin{aligned} F &= F(T, \{n_i\}, \{m_i\}) \\ &= \Omega_0(T, \{\mu_i^*\}, \{m_i\}) + \sum_i \mu_i^* n_i. \end{aligned} \quad (1)$$

where μ_i^* the effective chemical potential of particle type i , and Ω_0 is the thermodynamic potential density of a system comprised of free particles, which should be considered as an intermediate variable rather than a real one. The corresponding differential equation of Eq. (1) then becomes

$$dF = \frac{\partial \Omega_0}{\partial T} dT + \sum_i \mu_i^* dn_i + \sum_i \frac{\partial \Omega_0}{\partial m_i} dm_i, \quad (2)$$

where the differential of m_i is as follows:

$$dm_i = \sum_j \frac{\partial m_i}{\partial n_j} dn_j + \frac{\partial m_i}{\partial T} dT. \quad (3)$$

Then, we have

$$\begin{aligned} dF &= \left[\frac{\partial \Omega_0}{\partial T} + \sum_i \frac{\partial \Omega_0}{\partial m_i} \frac{\partial m_i}{\partial T} \right] dT \\ &+ \sum_i \left[\mu_i^* + \sum_j \frac{\partial \Omega_0}{\partial m_j} \frac{\partial m_j}{\partial n_i} \right] dn_i. \end{aligned} \quad (4)$$

The fundamental thermodynamic differential relations of free energy are

$$d\bar{F} = -\bar{S}dT - PdV + \sum_i \mu_i dN_i, \quad (5)$$

where \bar{F} , \bar{S} , N_i , P , V , and μ_i represents the free energy, entropy, particle number, pressure, volume, and chemical potential of the system, respectively. For a uniform system, we can define the free energy density $F = \bar{F}/V$, entropy density $S = \bar{S}/V$, and particle number density $n_i = N_i/V$. Substituting those into Eq. (5), we have

$$\begin{aligned} dF = & -SdT + \sum_i \mu_i dn_i \\ & + \left(-P - F + \sum_i \mu_i n_i \right) \frac{dV}{V}. \end{aligned} \quad (6)$$

Comparing Eq. (4) and Eq. (6), we obtain the following thermodynamic relationships,

$$S = -\frac{\partial \Omega_0}{\partial T} - \sum_i \frac{\partial \Omega_0}{\partial m_i} \frac{\partial m_i}{\partial T}, \quad (7)$$

$$\mu_i = \mu_i^* + \sum_j \frac{\partial \Omega_0}{\partial m_j} \frac{\partial m_j}{\partial n_i}, \quad (8)$$

$$P = -F + \sum_i \mu_i n_i. \quad (9)$$

Based on $F = \Omega_0 + \sum \mu_i^* n_i = \Omega + \sum \mu_i n_i$, the relationship between intermediate variables Ω_0 and true thermodynamic potential Ω is

$$\Omega = \Omega_0 - n_b \sum_j \frac{\partial \Omega_0}{\partial m_j} \frac{\partial m_j}{\partial n_b}. \quad (10)$$

Substituting Eq. (1) and Eq. (10) to Eq. (9),

$$P = -\Omega_0 + n_b \sum_j \frac{\partial \Omega_0}{\partial m_j} \frac{\partial m_j}{\partial n_b} = -\Omega \quad (11)$$

demonstrated the consistency of the entire process.

The energy density is given by

$$E = F + TS = \Omega_0 + \sum_i \mu_i^* n_i + TS. \quad (12)$$

Substituting Eq. (9) to Eq. (12), we have

$$E = -P + \sum_i \mu_i n_i + TS, \quad (13)$$

so the Euler equation for bulk strange quark matter is validated.

According to $F(T, \{n_i\}, \{m_i\}) = \Omega_0(T, \{\mu_i^*\}, \{m_i\}) + \sum \mu_i^* n_i$, there is $\partial F / \partial \mu_i^* = \partial \Omega_0 / \partial \mu_i^* + n_i = 0$. The particle number densities is

$$n_i = -\frac{\partial \Omega_0}{\partial \mu_i^*}. \quad (14)$$

III. DENSITY AND/OR TEMPERATURE DEPENDENT PARTICLE MASSES

The main research idea of the model is to simulate the interactions between quarks by using baryon density-dependent quark masses. And the corresponding quarks behave as free particles with equivalent masses. This idea was initially proposed by Fowler and further developed by Chakrabarty [46, 47], namely

$$m_i = m_{i0} + \frac{B}{3n_b}, \quad (15)$$

where m_{i0} , B and n_b are the current mass ($m_{u0} = 2.16$ MeV, $m_{d0} = 4.70$ MeV, and $m_{s0} = 93.5$ MeV) [48], bag constant and baryon number density.

Afterwards, the temperature contribution is taken into account in the mass scale [49], i.e.

$$m_i = m_{i0} + \frac{B}{3n_b} \left[1 - \left(\frac{T}{T_c} \right)^2 \right], \quad (16)$$

where T_c is the critical temperature for the transition of hadronic matter into QGP.

In order to better reflect the interactions between quarks, Peng et al. derived a scaling that is inversely proportional to the cubic root of the baryon number density based on the in-medium chiral condensates and linear confinement [45, 50], i.e.,

$$m_i = m_{i0} + \frac{D}{n_b^{1/3}}, \quad (17)$$

where D represents the strength of confinement interaction. Using a similar derivation, the scaling was extended to finite temperature as [39]

$$m_i = m_{i0} + \frac{D}{n_b^{1/3}} \left[1 - \frac{8T}{\lambda T_c} \exp \left(-\frac{\lambda T_c}{T} \right) \right], \quad (18)$$

where the constant $\lambda = 1.6$, and $T_c = 175$ MeV is the critical temperature at the deconfinement phase transition.

Further, considering the contribution of one-gluon-exchange and perturbation interactions, the scaling was obtained at zero temperature [3, 51], i.e.

$$m_i = m_{i0} + \frac{D}{n_b^{1/3}} + C n_b^{1/3}, \quad (19)$$

where C represents the strength of one-gluon-exchange and perturbation interactions.

Similarly, taking into account the temperature, the scaling becomes [52]

$$\begin{aligned} m_i = & m_{i0} + \frac{D}{n_b^{1/3}} \left(1 + \frac{8T}{\Lambda} e^{-\Lambda/T} \right)^{-1} \\ & + C n_b^{1/3} \left(1 + \frac{8T}{\Lambda} e^{-\Lambda/T} \right), \end{aligned} \quad (20)$$

where $\Lambda = \lambda T_c = 280$ MeV. For above formula, the part of interaction mass tends to zero above the critical temperature T_c , which conforms to the characteristics of asymptotic freedom.

At finite temperatures, it is necessary to know the effective mass of gluons because their contribution cannot be ignored. Based on Borsányi *et al.*'s lattice simulation, which provided 48 pressure values [53], we obtained a fitting result for the effective mass of the gluon [54]. Define the scaling temperature as $x = T/T_c$. For $T < T_c$, the effective mass of gluons is

$$\frac{m_g}{T} = \sum_i a_i x^i = a_0 + a_1 x + a_2 x^2 + a_3 x^3, \quad (21)$$

where $a_0 = 67.018$, $a_1 = -189.089$, $a_2 = 212.666$, $a_3 = -83.605$. For $T > T_c$, the gluon's equivalent mass is

$$\frac{m_g}{T} = \sum_i b_i \alpha^i = b_0 + b_1 \alpha + b_2 \alpha^2 + b_3 \alpha^3, \quad (22)$$

where expansion coefficients $b_0 = 0.218$, $b_1 = 3.734$, $b_2 = -1.160$, $b_3 = 0.274$, and α is the strong coupling constant, which is running and depends on the solution of the renormalization group equation. Recently, we solved the renormalization group equations for QCD couplings by a new mathematical idea and obtained a fast convergent expression for α [55], where the leading order term is

$$\alpha = \frac{\beta_0}{\beta_0^2 \ln(u/\Lambda) + \beta_1 \ln \ln(u/\Lambda)}, \quad (23)$$

where $\beta_0 = 11/2 - N_f/3$, $\beta_1 = 51/4 - 19N_f/12$, where the number of flavors $N_f = 3$. The renormalization scale varies linearly with temperature as $u/\Lambda = c_0 + c_1 x$, $c_0 = 1.054$, $c_1 = 0.479$.

IV. PROPERTIES OF STRANGE QUARK MATTER

The SQM is assumed to consist of quarks, gluons, and leptons at finite temperature, but only quarks and electrons at zero temperature. Based on the baryon density-dependent quark mass model, the contribution of thermodynamics potential density for free particles is

$$\Omega_0 = \Omega_0^+ + \Omega_0^- + \Omega_0^g. \quad (24)$$

The contribution of particle (+) and antiparticle (-) are

$$\Omega_0^\pm = \sum_i -\frac{d_i T}{2\pi^2} \int_0^\infty \ln \left[1 + e^{-(\sqrt{p^2+m_i^2} \mp \mu_i^*)/T} \right] p^2 dp, \quad (25)$$

where $d_i = 3(\text{colors}) \times 2(\text{spins}) = 6$ for $i = u, d, s$, $d_i = 2$ for $i = e, \mu$, and $d_i = 1$ for $i = \nu_e, \nu_\mu$.

The contribution of gluon is

$$\Omega_0^g = \frac{d_g T}{2\pi^2} \int_0^\infty \ln \left[1 - e^{-\sqrt{p^2+m_g^2}/T} \right] p^2 dp, \quad (26)$$

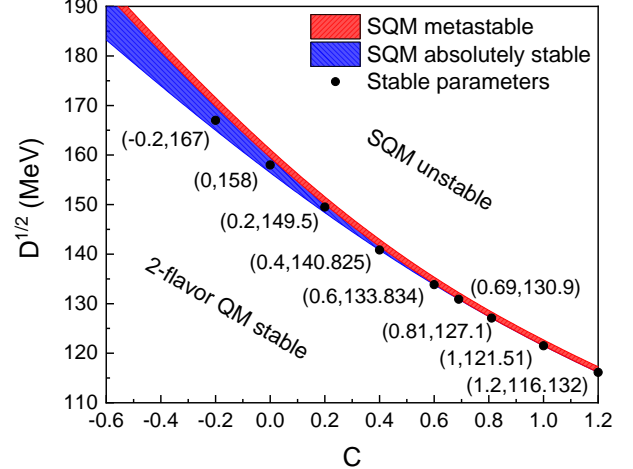


FIG. 1. The stability window for the baryon density-dependent quark mass model.

where $d_g = 8(\text{colors}) \times 2(\text{spins}) = 16$.

The number density of particle and anti-particle are

$$n_i^\pm = -\frac{\partial \Omega_0^\pm}{\partial \mu_i^*} = \frac{d_i}{2\pi^2} \int_0^\infty \frac{p^2 dp}{e^{(\sqrt{p^2+m_i^2} \mp \mu_i^*)/T} + 1}. \quad (27)$$

At the zero temperature, the contribution of thermodynamic potential density for free particles is

$$\Omega_0 = -\sum_i \frac{d_i}{24\pi^2} \left[\mu_i^* \nu_i (\nu_i^2 - \frac{3}{2} m_i^2) + \frac{3}{2} m_i^4 \ln \frac{\mu_i^* + \nu_i}{m_i} \right], \quad (28)$$

where $\nu_i = \sqrt{\mu_i^{*2} - m_i^2}$ is the Fermi momentum of particle.

The number density of particle and anti-particle at the zero temperature are

$$n_i = -\frac{\partial \Omega_0}{\partial \mu_i^*} = \frac{d_i \nu_i^3}{6\pi^2}. \quad (29)$$

All other thermodynamic quantities can be obtained by substituting the thermodynamic potential density into Eqs. (7)-(12).

In order to be consistent with the conventional nuclear physics and to ensure the stable existence of strange quark stars in the Universe, the confinement parameter D and perturbative parameter C should satisfy the condition that the energy per baryon of strange quark matter is less than 930 MeV at zero temperature and pressure, while that of ud quark matter larger than 930 MeV. Furthermore, strange quark matter with a minimum energy per baryon larger than 930 MeV and less than 939 MeV is metastable. Based on the above conditions, we obtain a stability window consisting of the confinement parameter $D^{1/2}$ and perturbative parameter C , as shown in Fig. 1, where the blue and red regions are absolute stable and metastable SQMs, respectively. In this work, we adopt the parameter set $(C, \sqrt{D}$ in MeV) as $(0.69, 130.9)$.

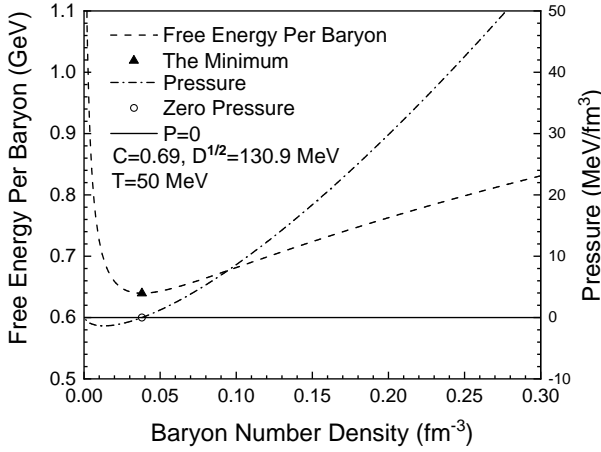


FIG. 2. The relationship between the free energy per baryon, pressure and density at $T = 50$ MeV, where $D^{1/2} = 130.9$ MeV and $C = 0.69$.

To test the self-consistency of the thermodynamic treatment more intuitively, the thermodynamic test equation is generally defined as [45]

$$P - n^2 \frac{d}{dn} \left(\frac{F}{n} \right) = 0. \quad (30)$$

The free energy per baryon and the corresponding pressure at $T = 50$ MeV are shown in Fig. 2. The triangle is the minimum free energy per baryon, and the open circles correspond to the zero pressure. We notice that the pressure is zero when the density is at the lowest free energy per baryon, which is a necessary condition for thermodynamic consistency and consistent with the test equation Eq. (30).

V. EVOLUTION OF STRANGE QUARK STARS

For the description of the matter inside strange quark stars, leptons must be also taken into account. Due to the weak reactions such as $d, s \leftrightarrow u + e + \bar{\nu}_e$, $s + u \leftrightarrow u + d$ and $e \leftrightarrow \mu + \nu_e + \bar{\nu}_\mu$, the chemical potential μ_i ($i = u, d, s, e$) needs to satisfy weak equilibrium conditions

$$\mu_u^* + \mu_e - \mu_{\nu_e} = \mu_d^* = \mu_s^*, \quad (31)$$

and

$$\mu_e = \mu_\mu + \mu_{\nu_\mu} - \mu_{\nu_\mu}. \quad (32)$$

The charge neutrality condition is

$$2n_u - n_d - n_s - 3n_e - 3n_\mu = 0, \quad (33)$$

where the particle number densities $n_i = n_i^+ - n_i^-$.

In addition, the quark number density satisfies the baryon number conservation condition

$$n_b = \sum_{q=u,d,s} \frac{1}{3} (n_q^+ - n_q^-). \quad (34)$$

The paper studies the evolution of properties of strange quark stars, including neutrino-trapping, deleptonization, neutrino-transparent, and the formation of a cold strange quark star.

Proto-neutrinos are trapped in the early stages of a strange quark star with an unshocked and low entropy ($S/n_b \sim 1$) core, known as the neutrino-trapped phase, during which the lepton fraction remains constant. The lepton fraction during neutrino-trapped phase is

$$Y_{L,e} = \frac{n_e + n_{\nu_e}}{n_b} = \xi, \quad (35)$$

$$Y_{L,\mu} = \frac{n_\mu + n_{\nu_\mu}}{n_b} = 0, \quad (36)$$

where $\xi \simeq 0.4$ depends on the efficiency of electron capture reactions in the early neutrino-trapped phase, which is the initial time $t \sim 0$ s before the supernova explosion [56], $Y_{L,\mu}$ means the fact that there are no muons in matter when neutrinos are captured [57].

Then, with approximately $0.5 - 1$ s after the core bounce of a star, the explosion and shock wave of a stellar supernova lift off the stellar envelope. If a supernova explosion causes an extensive loss of neutrinos and deleptonization, leading to the extensive loss of lepton pressure, an increase in entropy per baryon and mantle collapse, i.e. $S/n_b \sim 1.5$ and $\xi \simeq 0.2$, accretion becomes less important, and the star will continue to evolve. If the intensity of the supernova explosion is not strong enough to cause the outer mantle of proto-strange quark stars to undergo deleptonization, the matter will gather again, leading to the formation of a black hole. This study considers the first scenario.

In the next $10 - 15$ s, the star undergoes neutrino diffusion, deleptonization, and core heating. The star begins to rapidly lose neutrinos, with a maximum entropy per baryon $S/n_b = 2$ in the core and the neutrino fraction Y_{ν_e} reaching 0, and the equation of state will soften. If the gravitational pressure is large enough, a black hole could form. In this study, we assume that strange quark stars evolves to the final stage to form a cold catalytic strange quark star, and no black hole is formed during its evolution.

After deleptonization, the core of the hot strange quark star undergoes thermal diffusion and cooling. After about 50 s, as the average energy of neutrinos decreases, the neutrinos in the star become essentially transparent, and the core reaches a cold catalytic configuration. Then the core continues to cool through thermal radiation, and finally, it shrinks to a catalysed cold strange quark star at $T = 0$ MeV.

In Fig. 3, we show the relative fraction of particles of the matter inside strange quark stars as functions of baryon density at various snapshots along its evolution, from birth ($S/n_b = 1, Y_{L,e} = 0.4$) to cold-catalyzed strange quark stars at $T = 0$ MeV. The upper and lower panels correspond to the neutrino-trapped and neutrino-transparent stage, respectively. From the first stage to

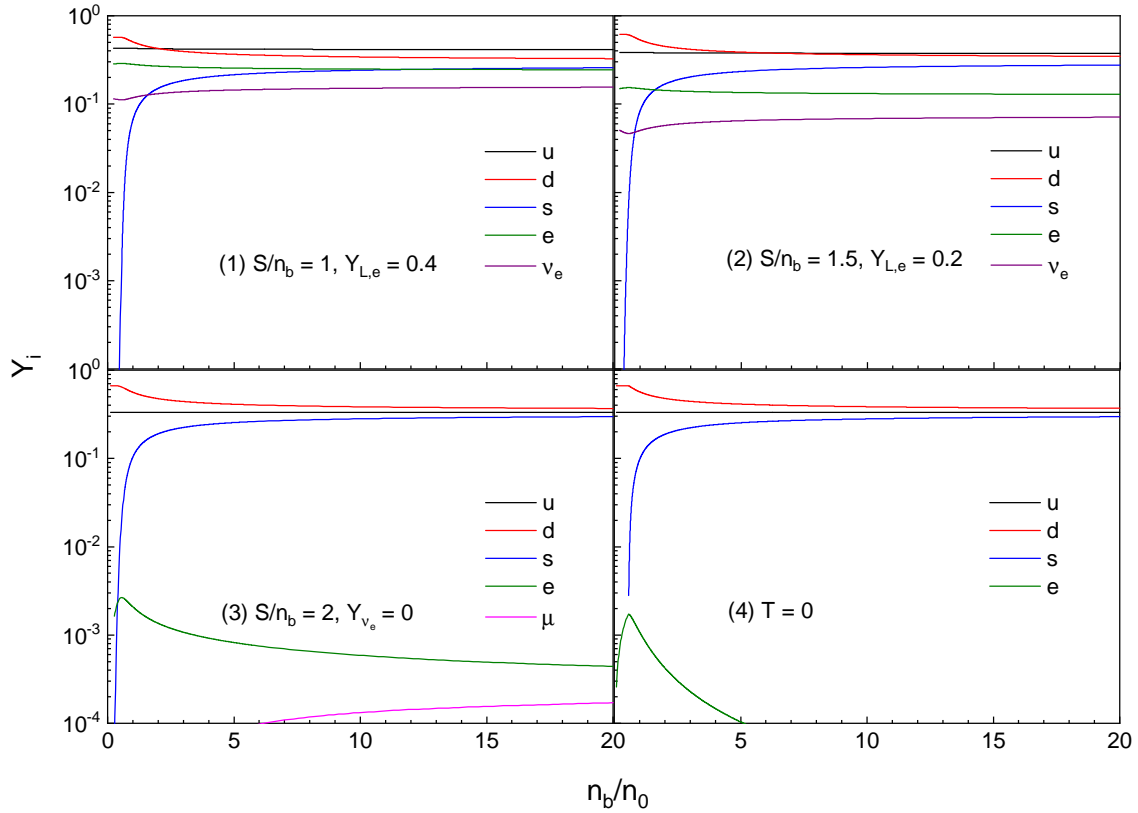


FIG. 3. The relative particle fraction of the matter inside of strange quark stars as functions of baryon density at various snapshots of its evolution. The upper and lower panels are correspond to the neutrino-trapped and neutrino-transparent stage, respectively.

the second stage, we observe that higher neutrino concentrations increase the relative abundance of u quarks while decreasing that of d and s quarks, leading to the emergence of s quarks at higher n_b . In other words, the higher neutrino concentrations implies lower abundances of d and s quark and later appearance of s quarks. This is consistent with some studies on the evolution of proto-neutron stars [57, 58]. For instance, research has shown that higher neutrino concentrations during the evolution of proto-neutron stars delay the emergence of particles with strangeness [57, 58]. Correspondingly, along the evolution lines of the star, the higher probabilities of s quark correlate with the softer EOS, means the lower maximum masses of star. This will be validated in the research of mass-radius relation of strange quark stars. In addition, in the fourth stage, due to the chemical potential always being smaller than the particle mass, the number of μ is zero at $T = 0$ MeV.

The equation of state of SQM at different stages of evolution of SQS is shown in Fig. 4. It is clearly visible that the strange quark stars with lower neutrino concentrations exhibit a soft EoS, meaning lower pressure at the same energy density. This is because the probability of s quarks appearing in the matter inside of strange quark stars increases with the deleptonization of evolution of star. At the same time, this also indicates that the max-

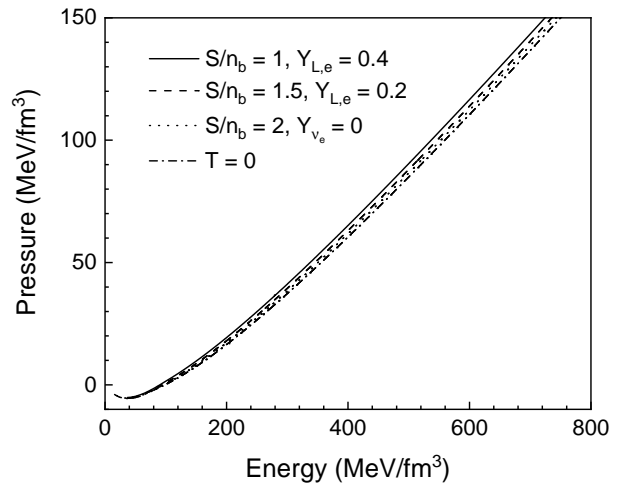


FIG. 4. The relationship between the pressure and energy density at different stages of evolution of SQS.

imum mass of a star will decrease when it evolves from the neutrino-trapped stage to the neutrino-transparent stage, which will be verified in the subsequent mass radius relationship.

In Fig. 5, we show the relationship between the tem-

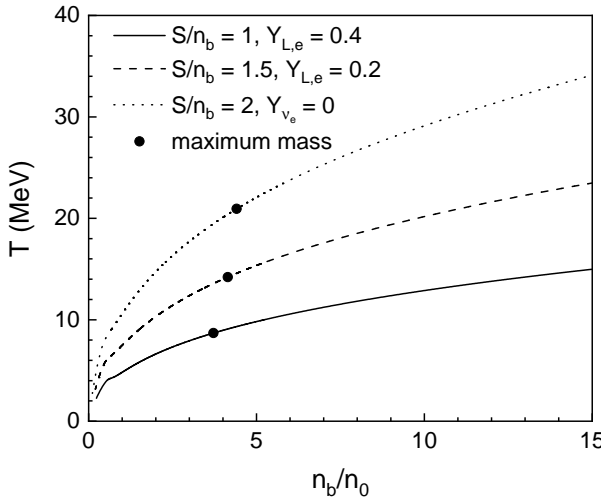


FIG. 5. The temperature as a function of baryon number density at different stages of evolution of SQS.

perature and baryon number density at different stages of evolution of SQS, where the black dots correspond to the core temperature of the matter inside strange quark stars. It can be seen that the temperatures in the first phase are relatively low and below 15 MeV in most density ranges, which is the result of stellar collapse and core bounce. The baryon number density and temperature at the core of the most massive star are $3.72n_0$ and 8.69 MeV. In the second stage, the temperatures rises and remains below 23 MeV in most density ranges. This is due to neutrino emission and matter accretion, leading to deleptonization and an increase in the entropy density per baryon. The baryon number density and temperature at the core of the most massive star are $4.14n_0$ and 14.21 MeV. In the third stage, the temperature rises further and remains below 34 MeV in most density ranges due to the maximum heating of stellar matter by neutrino emission. The baryon number density and temperature at the core of the most massive star are $4.41n_0$ and 20.94 MeV. Subsequently, the core is continuously cooled by thermal radiation and reaches $T = 0$ MeV after about 100 years. In addition, the temperature of a strange quark star is lower than that of its corresponding hadron star [56, 58], which allows us to determine the composition of compact objects by observing the evolution of surface temperature.

Based on the EOSs, we solve the Tolman-Oppenheimer-Volkov equation

$$\frac{dP}{dr} = -\frac{GmE}{r^2} \frac{(1+P/E)(1+4\pi r^3 P/m)}{1-2Gm/r}, \quad (37)$$

and

$$dm = 4\pi Er^2 dr. \quad (38)$$

The mass-radius relation for strange quark stars at different stages of evolution of SQS are shown in Fig. 6,

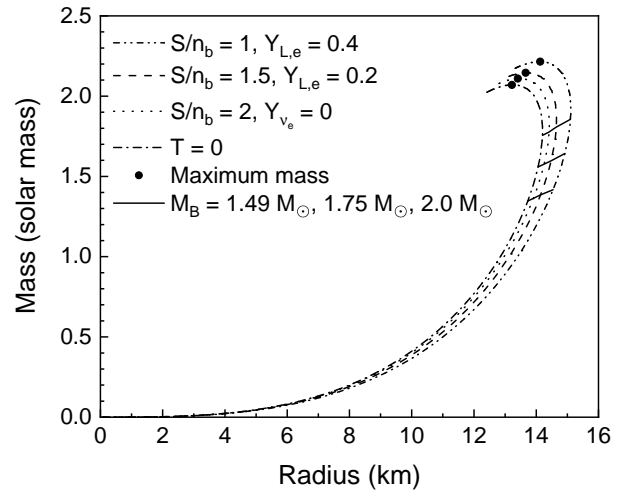


FIG. 6. The mass-radius relationship for strange quark stars at different stages of evolution of SQS.

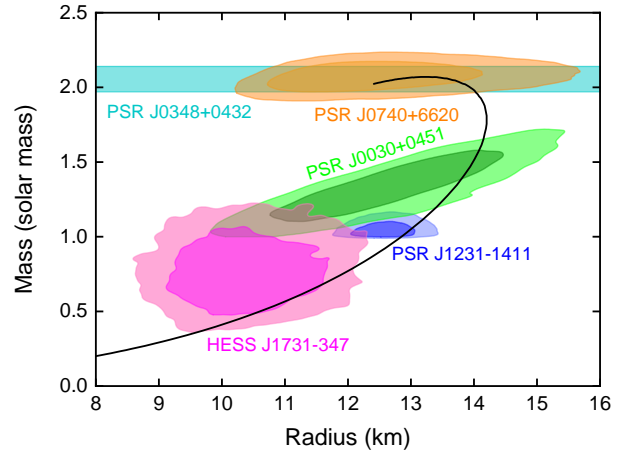


FIG. 7. The mass-radius relationship for strange quark stars at $T = 0$, where $D^{1/2} = 130.9$ MeV and $C = 0.69$.

where the most massive stars are represented by black dots. We can see that the maximum mass and corresponding radius of strange quark stars gradually decrease when it evolves from the neutrino-trapped stage to the neutrino-transparent stage. The maximum mass and corresponding radius of strange quark stars are $2.21 M_\odot$ and 14.13 km at the first stage of the neutrino-trapped process, the maximum mass and corresponding radius of strange quark stars are $2.15 M_\odot$ and 13.66 km at the second stage of the neutrino-trapped process, the maximum mass and corresponding radius of strange quark stars are $2.11 M_\odot$ and 13.41 km at the third stage of the neutrino-transparent process, and the maximum mass and corresponding radius of stable strange quark stars are $2.07 M_\odot$ and 13.22 km at zero temperature. The maximum mass of strange quark stars in each stage exceeds $2 M_\odot$. The decrease in the maximum mass of strange quark star is consistent with the softening of the equation of state in

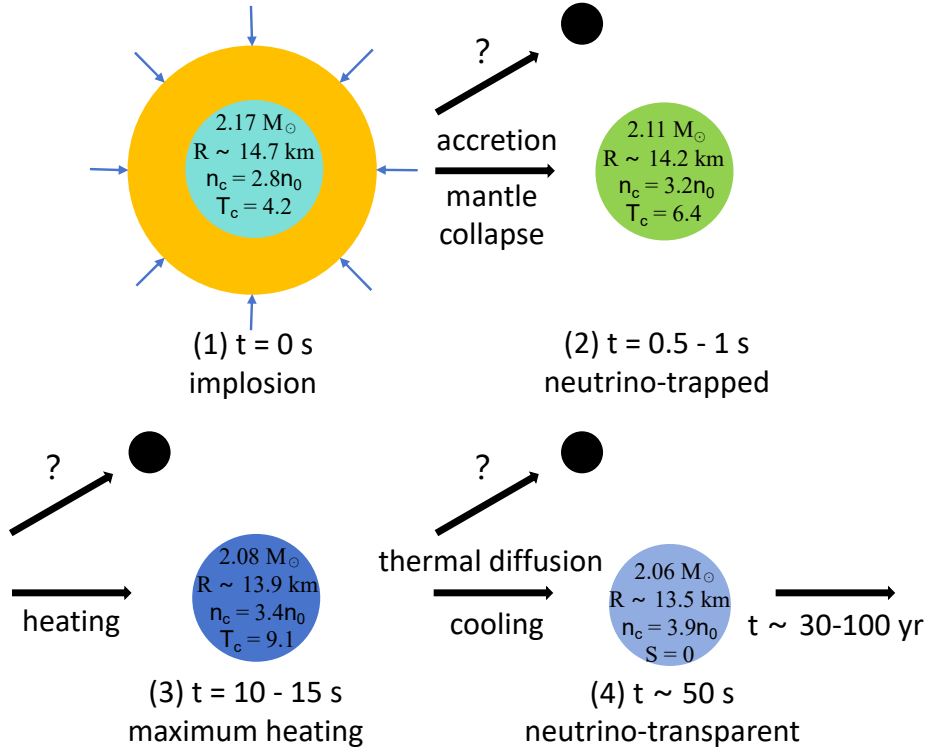


FIG. 8. The schematic diagram of the state of different temporal stages in the evolution of proto-strange quark stars to strange quark stars at a fixed baryon-mass $M_B = 2.4 M_\odot$.

Fig. 4 as it evolves. In addition, we also presented strange quark stars with baryon masses $M_B = 2.0, 1.75, 1.49 M_\odot$ in each stage, and found that the evolution of strange quark star with constant baryon masses is approximately shown as a straight line in the figure.

The mass-radius relationship for strange quark stars at $T = 0$ are shown in Fig. 7. We have also included 2-D marginalized posteriors of masses and radii of Hess J1731-347 [59], PSR J0030+0451 [60], PSR J1231+1411 [61, 62], and PSR J0740+6620 [63]. The contours in the 2-D marginalized posterior denote the 68% and 95% credible intervals. In addition, the lower and upper limits of the masses and radii of PSR J0348+0432 [64] were also included. It can be seen that the results of the strange quark star with $C = 0.69$ and $D^{1/2} = 130.9$ MeV are consistent with the observational mass and radius of Hess J1731-347, PSR J1231-1411, PSR J0030+0451, PSR J0348+0432, and PSR J0740+6620. The most interesting aspect of the SQSs model is that it describes compact stars with masses up to approximately $1.5 M_\odot$ and radii between 8 – 12 km, such as PSR J0030+0451 and Hess J1731-347, which can explain the observation results of some cold, dense, and small compact stars that do not conform to the standard NSs model.

Based on the above analysis, we provide a schematic diagram in Fig. 8, illustrating the state of different tempo-

ral stages in the evolution of proto-strange quark stars to strange quark stars at a fixed baryon-mass. The baryon-mass is given by [57]

$$M_B = m_n \int_0^R \frac{4\pi r^2 n(r)}{[1 - 2Gm(r)/r]^{1/2}} dr. \quad (39)$$

At fixed $M_B = 2.4 M_\odot$, the gravitational mass and radius decrease, while the baryon density and temperature at the core increase as the star evolves, reaching a stable state at $T = 0$ in about 100 years later.

VI. SUMMARY

We studied the properties of strange quark matter and revealed the evolution process during the evolution of strange quark stars by given a self consistent thermodynamic treatment method.

It is found that higher neutrino concentrations in early stage increase the relative abundance of u quarks while decreasing that of d and s quarks, leading to the emergence of s quarks at higher n_b . This is consistent with some studies on the evolution of proto-neutron stars. Based on the equation of state of the matter inside of strange quark stars, it can be seen that the strange quark stars with lower neutrino concentrations correspond to a soft EoS because the probability of s quarks

increases, meaning the maximum mass of a star will decrease when it evolves from the neutrino-trapped stage to the neutrino-transparent stage. In the study of temperature on the distribution of baryon number density in the first three stages, we can see that the temperatures in the first phase are low relatively and below 15 MeV in most density ranges due to stellar collapse and core bounce, the temperatures in the second stage rises and remains below 23 MeV in most density ranges due to neutrino emission and matter accretion, leading to deleptonization and an increase in the entropy density per baryon, the temperature in the third stage rises further and remains below 34 MeV in most density ranges due to the maximum heating of stellar matter by neutrino emission. Subsequently, the core is continuously cooled by thermal radiation and reaches $T = 0$ MeV after about 100 years. In addition, the temperature of a strange quark star is lower than that of its corresponding hadron star, which allows us to determine the composition of compact objects by observing the function of temperature.

Based on the EOSs, we obtained the mass-radius relationship of the strange quark stars at different stages of evolution of SQS. It can be seen that the maximum mass and corresponding radius of strange quark stars gradually decrease along the evolution of stars. The maximum mass and corresponding radius of strange quark stars are $2.21 M_{\odot}$ and 14.13 km at the first stage, the maximum mass and corresponding radius of strange quark stars are $2.15 M_{\odot}$ and 13.66 km at the second stage, the maximum mass and corresponding radius of strange quark stars are $2.11 M_{\odot}$ and 13.41 km at the third stage, and the maximum mass and corresponding radius of stable strange

quark stars are $2.07 M_{\odot}$ and 13.22 km at zero temperature. The maximum mass of strange quark stars in each stage exceeds $2 M_{\odot}$. The decrease in the maximum mass of strange quark star is consistent with the softening of the equation of state as it evolves. In addition, we found that the mass-radius relationship of the cold strange quark star with $C = 0.69$ and $D^{1/2} = 130.9$ MeV are consistent with the observational mass and radius of Hess J1731-347, PSR J1231-1411, PSR J0030+0451, PSR J0348+0432, and PSR J0740+6620, which can explain the observation results of some cold, dense, and small compact stars that do not conform to the standard NSs model. Finally, we provide a schematic diagram, illustrating the state of different stages along the evolution of stars at a fixed baryon-mass. It found that the gravitational mass and radius decrease, while the baryon density and temperature at the core increase as the star evolves, reaching a stable state at $T = 0$ in about 100 years later.

ACKNOWLEDGMENTS

The authors would like to thank support from NSFC (Nos. 11135011, 12275234, 12375127), the Natural Science Foundation of Fujian Province (No. 2024J01319), the Young and Middle-aged Teachers' Educational Research Project of Fujian Province (No. JAT231123), the Scientific Research Start-up Foundation of Wuyi University (No. YJ202212), and the national SKA programme (No. 2020SKA0120300).

[1] A. R. Bodmer, Phys. Rev. D 4, 1601 (1971).
[2] E. Witten, Phys. Rev. D 30, 272 (1984).
[3] C. J. Xia, G. X. Peng, S. W. Chen, Z. Y. Lu, and J. F. Xu, Phys. Rev. D 89, 105027 (2014).
[4] J. Sedaghat, G. H. Bordbar, M. Haghghat, and S. M. Zebarjad, Eur. Phys. J. C 85, 283 (2025).
[5] H. M. Chen, X. W. Li, C. J. Xia, and G. X. Peng, Phys. Rev. D 109, 054013 (2024).
[6] G. Lugones and A. G. Grunfeld, Phys. Rev. D 107, 043025 (2023).
[7] J. Rafelski, Ch. Dietl, and L. Labun, Acta Phys. Polon. B 43, 2251 (2012).
[8] J. Rafelski, L. Labun, and J. Birrell, Phys. Rev. Lett. 110, 111102 (2013).
[9] L. W. Piotrowski, K. Małek, L. Mankiewicz, M. Sokołowski, G. Wrochna, A. Zadrożny, and A. F. Żarnecki, Phys. Rev. Lett. 125, 091101 (2020).
[10] ANTARES Collaboration, JCAP 01, 012 (2023).
[11] H. M. Chen, C. J. Xia, and G. X. Peng, Phys. Rev. D 109, 054031 (2024).
[12] H. S. You, H. M. Chen, J. F. Xu, C. J. Xia, R. X. Xu, and G. X. Peng, Phys. Rev. D 109, 034003 (2024).
[13] G. Lugones and A. G. Grunfeld, Universe 10, 233 (2024).
[14] E. Farhi and R. L. Jaffe, Phys. Rev. D 30, 2379 (1984).
[15] H. M. Chen and C. J. Xia and G. X. Peng, Chin. Phys. C 46, 055102 (2022).
[16] J. F. Xu, Y. A. Luo, L. Li, and G. X. Peng, Phys. Rev. D 96, 063016 (2017).
[17] Z. Zhang, P. C. Chu, X. H. Li, H. Liu and X. M. Zhang, Phys. Rev. D 103, 103021 (2021).
[18] K. S. Cheng, Z. G. Dai, and T. Lu, Int. J. Mod. Phys. D 7, 139 (1998).
[19] M. A. Perez-Garcia, J. Silk, and J. R. Stone, Phys. Rev. Lett. 105, 141101 (2010).
[20] C. Alcock, E. Farhi, and A. Olinto, Astrophys. J. 310, 261 (1986).
[21] A. V. Olinto, Phys. Lett. B 192, 71 (1987).
[22] M. Herzog and F. K. Ropke, Phys. Rev. D 84, 083002 (2011).
[23] D. D. Ivanenko and D. F. Kurdgelaidze, Astrophys. 1, 251 (1965).
[24] D. D. Ivanenko and D. F. Kurdgelaidze, Lett. Nuovo Cim. 2, 13 (1969).
[25] N. Itoh, Prog. Theor. Phys. 44, 291 (1970).
[26] A. Issifu, F. M. de Silva, and D. P. Menezes, Eur. Phys. J. C 84, 463 (2024).
[27] X. Y. Song, Phys. Rev. D 111, 063018 (2025).
[28] M. Alford, D. Blaschke, A. Drago, T. Klähn, G. Pagliara, and J. Schaffner-Bielich, Nature 445, E7 (2007).

- [29] J. J. Drake, H. L. Marshall, S. Dreizler, P. E. Freeman, A. Fruscione, M. Juda, V. Kashyap, F. Nicastro, D. O. Pease, B. J. Wargelin, and K. Werner, *Astrophys. J.* 572, 996 (2002).
- [30] P. O. Slane, D. J. Helfand, and S. S. Murray, *Astrophys. J. Lett.* 571, L45 (2002).
- [31] M. JU, P. C. Chu, X. H. Wu, and H. Liu, *Eur. Phys. J. C* 85, 40 (2025).
- [32] T. C. Chan, K. S. Cheng, T. Harko, H. K. Lau, L. M. Lin, W. M. Suen, and X. L. Tian, *Astrophys. J.* 695, 732 (2009).
- [33] M. Yuan, J. G. Lu, Z. L. Yang, X. Y. Lai, and R. X. Xu, *Res. Astron. Astrophys.* 17, 92 (2017).
- [34] R. Ouyed, M. Kostka, N. Koning, D. A. Leahy, and W. Steffen, *Mon. Not. R. Astron. Soc.* 423, 1652 (2012).
- [35] H. T. Janka, F. Hanke, L. Hüdepohl, A. Marek, B. Müller, and M. Obergaulinger, *Prog. Theor. Exp. Phys.* 2012, 01A309 (2012).
- [36] T. Fischer, D. Blaschke, M. Hempel, T. Klahn, R. Lastowiecki, M. Liebendörfer, G. Martínez-Pinedo, G. Pagliara, I. Sagert, F. Sandin, J. Schaffner-Bielich, and S. Typel, *Phys. Atom. Nucl.* 75, 613 (2012).
- [37] P. C. Chu, H. Liu, H. M. Liu, X. H. Li, X. H. Wu, and Y. Zhou, *Phys. Rev. D* 110, 123031 (2024).
- [38] J. Sedaghat, B. E. Panah, R. Moradi, S. M. Zebarjad, and G. H. Bordbar, *Eur. Phys. J. C* 84, 171 (2024).
- [39] X. J. Wen, X. H. Zhong, G. X. Peng, P. N. Shen, and P. Z. Ning, *Phys. Rev. C* 72, 015204 (2005).
- [40] Y. Yang, C. Wu, and J. F. Yang, *Eur. Phys. J. C* 85, 426 (2025).
- [41] R. X. Xu, *Astrophys. J.* 596, L59 (2003).
- [42] G. X. Peng, *Europhys. Lett.* 72, 69 (2005).
- [43] J. F. Xu, G. X. Peng, F. Liu, D. F. Hou, and L. W. Chen, *Phys. Rev. D* 92, 025025 (2015).
- [44] O. G. Benvenuto and G. Lugones, *Phys. Rev. D* 51, 1989 (1995).
- [45] G. X. Peng, H. C. Chiang, B. S. Zou, P. Z. Ning, and S. J. Luo, *Phys. Rev. C* 62, 025801 (2000).
- [46] G. N. Fowler and S. Raha and R. M. Weiner, *Z. Phys. C* 9, 271 (1981).
- [47] S. Chakrabarty, *Phys. Rev. D* 48, 1409 (1993).
- [48] Particle Data Group, *Phys. Rev. D* 110, 030001 (2024).
- [49] Y. Zhang and R. K. Su, *Phys. Rev. C* 65, 035202 (2002).
- [50] G. X. Peng and H. C. Chiang and J. J. Yang and L. Li and B. Liu, *Phys. Rev. C* 61, 015201 (1999).
- [51] S. W. Chen and L. Gao and G. X. Peng, *Chin. Phys. C* 36, 947 (2012).
- [52] Z. Y. Lu and G. X. Peng and S. P. Zhang and M. Ruggieri and V. Greco, *Nucl. Sci. Tech* 27, 148 (2016).
- [53] Sz. Borsányi, and G. Endrődi and Z. Fodor and S. D. Katz and K. K. Szabo, *J. High. Energy. Phys.* 01, 138 (2012).
- [54] H. M. Chen, C. J. Xia, and G. X. Peng, *Phys. Rev. D* 105, 014011 (2022).
- [55] H. M. Chen and L. M. Liu and J. T. Wang and M. Waqas and G. X. Peng, *Int. J. Mod. Phys. E* 31, 2250016 (2022).
- [56] M. Prakash and I. Bombaci and M. Prakash and P. J. Ellis and J. M. Lattimer and R. Knorren, *Phys. Rep.* 280, 1 (1997).
- [57] M. Malfatti and M. G. Orsaria and G. A. Contrera and F. Weber and I. F. Ranea-Sandoval, *Phys. Rev. C* 100, 015803 (2019).
- [58] A. Issifu and K. D. Marquez and M. R. Pelicer and D. P. Menezes, *Mon. Not. R. Astron. Soc.* 522, 3263 (2023).
- [59] V. Doroshenko and V. Suleimanov and G. Pühlhofer and A. Santangelo, *Nat. Astron.* 6, 1444 (2022).
- [60] T. E. Riley et al., *Astrophys. J.* 887, L21 (2019).
- [61] T. Salmi et al., *Astrophys. J.* 976, 58 (2024).
- [62] L. Qi et al., *Astrophys. J.* 976, 58 (2024).
- [63] T. E. Riley et al., *Astrophys. J. Lett.* 918, L27 (2021).
- [64] J. Antoniadis et al., *Science* 340, 1233232 (2013).